Comparative Investigation of the Formation of Polytetrafluoroethylene Nanoparticles on Different Solid Substrates Through the Adsorption of Tetrafluoroethylene

Ashkan Garshasbi,[1] Mohammad Mahdi Doroodmand,[1,2] Reza Pooladi,[1,3,4] Afsaneh Safavi,[1,2] Mohammad Hossein Sheikhi[1]

[1]*Nanotechnology Research Institute, Shiraz University, Shiraz, Iran*
[2]*Department of Chemistry, College of Sciences, Shiraz University, Shiraz 71454, Iran*
[3]*Department of Element Engineering, College of Engineering, Shiraz University, Shiraz 71454, Iran*
[4]*Academic and Science Center, Kazerun, Iran*

Received 8 December 2009; accepted 3 September 2010
DOI 10.1002/app.33351
Published online 21 March 2011 in Wiley Online Library (wileyonlinelibrary.com).

ABSTRACT: The effects of different solid substrates, including carbon nanofibers (CNFs), activated carbon, alumina, silica, molecular sieves, and poly(*N*-vinylpyrrolidione) (PVP), were compared for the high-pressure synthesis of polytetrafluoroethylene [PTFE or $(CF_2)_n$] nanoparticles via the adsorption of thermally synthesized tetrafluoroethylene (C_2F_4) as the monomer. Scanning electron microscopy, Fourier transform infrared spectroscopy, and thermogravimetric analysis (TGA) were used for the characterization of the PTFE nanoparticles on different solid substrates. The results demonstrate that the average diameters of the PTFE nanoparticles were about 90 nm for the CNFs, 130 nm for PVP, 150 nm for alumina, and about 200 nm for silica. Also, TGA showed that the amounts of PTFE nanoparticles synthesized on each solid substrate were 3.53 ± 0.09% for CNFs, 2.31 ± 0.10% for PVP, 2.11 ± 0.12% for silica, and 0.97 ± 0.16% for alumina. Depending on the active surface area and the morphology of nanomaterials, such as CNFs, different capacities were evaluated for each solid support in the formation of the PTFE nanoparticles. The quantities and the size of the synthesized PTFE nanoparticles relied on the characteristics of the solid substrate. © 2011 Wiley Periodicals, Inc. J Appl Polym Sci 121: 2369–2377, 2011

Key words: adsorption; nanotechnology; radical polymerization

INTRODUCTION

Fluoropolymers are technical polymers with very special properties and applications.[1] These materials are among the most versatile plastics, thanks to their properties.[2] Thermal stability is the major feature of these polymers and spurs their applications where high temperature exposures in polymers are encountered.[3–5] The stability of fluoropolymers is derived mainly from their low polarizability and from their strong carbon–fluorine (C—F) bond energy, that is, 507 kJ/mol, compared to typical energies of 415 kJ/mol for C—H or 348 kJ/mol for C—C bonds. The most important fluoropolymer is polytetrafluoroethylene [PTFE or $(CF_2)_n$].[3]

PTFE has attracted much attention because of its excellent features, including its extreme thermal stability, low friction coefficients, considerable biocompatibility, dielectric constant, little moisture absorption, and chemical inertness. The special properties of PTFE come from its strong chemical bonding, the shielding of its carbon backbone by fluorine atoms, and the intermolecular interactions between its very long, helical $(CF_2)_n$ chains. These special chemical and structural features also give PTFE an extremely high melt viscosity ($\sim 10^9$ to 10^{11} kg m/s)[6] and a negligible solubility in all common solvents.[7] These unique characteristics have made PTFE a candidate in many widespread applications, such as in electronics,[8] mechanical engineering,[9] fuel cells,[10] aerospace,[11] chemical industries,[12] medical engineering,[13] food industry,[14] and so on.[15–17] The newest industrial applications of PTFE are its use as a matrix for polymer composites with a range of fillers as material coating,[18,19] superhydrophobic electrosprayed nanomaterials,[20] and electrolyte membranes.[21] These all reveal the industrial applications of PTFE and the importance of the applicable methods for the synthesis of PTFE.

Correspondence to: M. M. Doroodmand (doroodmand@shirazu.ac.ir).

Contract grant sponsor: Shiraz University Research Council, Tel: +098-711-6137363, Fax: +098-711-2286008.

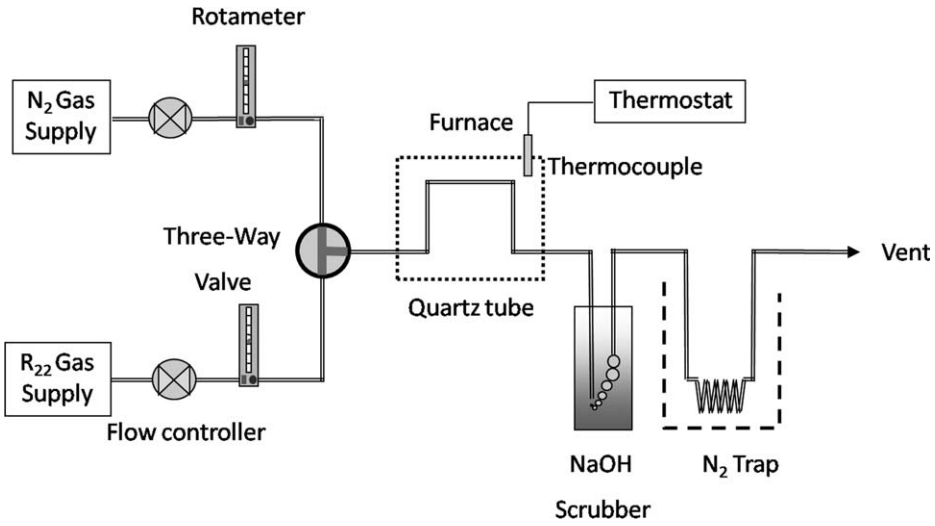

Figure 1 Schematic of the pyrolysis instrument for the synthesis and adsorption of TFE on different solid substrates.

For synthesis of PTFE, because of the problems related to the preparation of the monomer, the generated polymer is highly expensive.[22] To synthesize PTFE, tetrafluoroethylene (TFE or C_2F_4) as a monomer is generally produced via the pyrolysis of chlorofluoroparaffins, especially chlorodifluoromethane (i.e., $CHClF_2$, HCFC-22, or R22) at temperatures between 750 and 950°C. The most widely used process for the commercial production of TFE is the direct pyrolysis of R22.[23] The synthetic process used for PTFE formation is based on the radical polymerization mechanism in accordance with two different procedures.[24–28] The first procedure is founded on the direct gas-phase polymerization process, whereas the other procedure is anchored on the aqueous dispersion polymerization process.[24,27,28] Because a description of the gas phase synthesized polymer includes the size, shape, and morphology of PTFE,[29–31] in the synthetic processes of PTFE, the generated polymer should be well characterized through the controlled process parameters to yield PTFE particles for specific applications.[32]

One of the most important factors affecting the fantastic properties of the PTFE is the size of PTFE particles.[22] Recently, nanometer-sized PTFE particles have attracted much attention.[20,32] This is due to the unique physicochemical properties of PTFE nanoparticles.[18,32] Because the nanosize PTFE has some exceptional properties, such as excellent electrical resistance, chemical inertness, and mechanical and thermal stability, compared to bulky PTFE particles, PTFE nanoparticles play important roles in different parts of industry.[20,32] Therefore, despite the growing impact of the synthesis of PTFE particles, the introduction of controllable methods for the large-scale synthesis of PTFE nanomaterials is important.[6] In this study, a new method was used to synthesize PTFE nanoparticles/solid supports via adsorption of the TFE monomer on different solid substrates. In this study, the effects of the active surface area of the solid supports for controlling the amounts and size of the PTFE nanoparticles were also investigated in detail.

EXPERIMENTAL

Reagents and solutions

Gases, including $CHClF_2$ and nitrogen with 99.998 and 99.9% purity percentages, respectively, were purchased from ISCEON (London, England) and Parsbaloon (Shiraz, Iran), respectively. The silica (mean pore size = 80 Å, specific surface area ≈ 500 m^2/g), alumina (mean pore size = 60 Å, mean particle size = 0.20 μm), poly(*N*-vinylpyrrolidione) (PVP; weight-average molecular weight = 25,000 mol/g), and molecular sieves (mean pore size: 4 Å) were from Merck (Darmstadt, Germany).

Highly purified carbon nanofibers (CNFs), with a 250–400 nm internal diameter (specific surface area ≈ 850 m^2/g), and activated carbon were synthesized by the chemical vapor deposition method at temperatures to about 1300°C in an inert atmosphere of argon with acetylene gas (Parsbaloon) as a source of carbon and ferrocene (Merck) as a source of catalyst.

Apparatus

Pyrolysis system for the synthesis and direct adsorption of the monomer on the solid supports

The setup of the instrument is shown in Figure 1. The production line was quartz tubing (diameter = 8 mm, length ≈ 90 cm), which passed through a cubic furnace (Lenton, EF 11/8 and AF 11/6). R22 was selected as the source of monomer (TFE). The furnace (2500 W) was used for the pyrolysis of R22

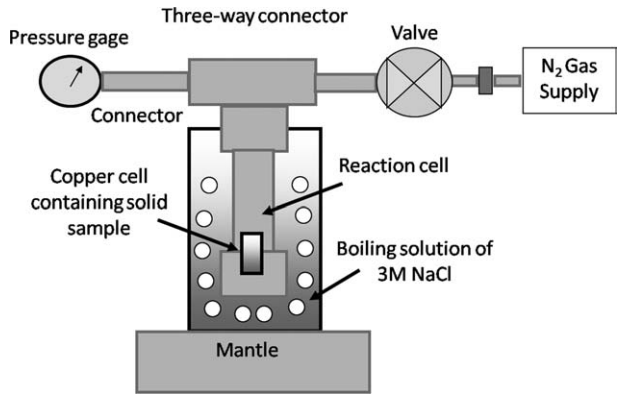

Figure 2 Schematic of the polymerization instrument for the synthesis of PTFE nanoparticles on different solid substrates.

and the production of TFE in an inert atmosphere of nitrogen. Mass flow controllers were used to control the flow rates of R22 and nitrogen gas before introduction into the quartz tubing. The generated TFE was than carried toward the end parts of the production line by the flow of nitrogen and bubbled into a 500-cm^3 vessel half filled with 5.0 mol/L NaOH. The outlet of the NaOH vessel was then connected to a glass U-trap (internal diameter = 0.5 cm, width = 3 cm, and height = 5 cm) located inside a vessel containing liquid nitrogen. Two valves (three-way) were also positioned at the two sides of the U-traps. Finally, the outlet of the U-trap was directed toward the hood through silicone tubing.

After the temperature of the furnace was set and the flow rates of R22 and nitrogen as diluents were optimized, these two gases were mixed and introduced into the quartz tubing. During the pyrolysis process, the synthesized TFE was then frozen inside the U-trap with liquid nitrogen. At the end of the experiment, the two valves were closed, and the U-trap was disconnected from the pyrolysis production line and joined to the other system used to adsorb the TFE on the solid supports.

In the adsorption process, suitable substrates, including the CNFs, silica, alumina, molecular sieves, and activated carbon, were put individually inside several glass traps (internal diameter = 0.5 cm, width = 3 cm, and height = 5 cm), connected sequentially to each other by silicone tubing. Then, the U-trap containing the frozen TFE was connected to the end of the array of traps with silicone tubing (internal diameter = 0.5 cm, length = 20 cm). During the adsorption process, we controlled the temperature of TFE inside the U-trap by locating it inside a refrigerator at a temperature of about −10°C.

In this study, scanning electron micrographs were obtained by scanning electron microscopy (SEM) instrumentation (XL-30 FEG scanning electron microscopy, Philips, 20 kV, Tehran, Iran). An atomic force microscopy (DME-SPM, version 2.0.0.9, Tehran, Iran) was also used for the atomic force microscopy (AFM) images. Spectroscopic methods, including Fourier transform infrared (FTIR) spectrometry (Shimadzu FTIR 8300 spectrophotometer, Shiraz, Iran) and patterned X-ray diffraction (XRD; D8, Advance, Bruker, axs, Shiraz, Iran), were used for the characterization of the PTFE nanoparticles. Thermogravimetric analysis (TGA, Shiraz, Iran) of the samples was also analyzed with a laboratory-made TGA instrument.

Apparatus system for the synthesis of the PTFE nanoparticles

The setup of the instrument for the synthesis of the PTFE nanoparticles on different solid supports is shown in Figure 2. It consisted of T-shape tubing (schedule no. 160, model 4F2, Shiraz, Iran). A pressure gauge was located at one of the end parts of the T-tubing, and the other end part of the T-tubing was connected to a nitrogen cylinder (0.22 m^3, 2×10^7 Pa) through a stainless steel valve to control the pressure of the reaction cell. The sidearm of the T-tubing (internal diameter = 4.0 cm, height = 15 cm) was used to locate the copper reaction cells (internal diameter = 0.5 mm, height = 3 cm) containing each type of solid substrate, adsorbed with TFE for the synthesis of the PTFE nanoparticles. To control the temperature of the reaction for the synthesis of the PTFE nanoparticles, the sidearm of the T-tubing was then located inside a beaker containing a solution of about 3.0 mol/L NaCl heated to about 100°C.

Procedure

For synthesis of TFE on the solid substrates, the temperature of the furnace was set to 950°C. The flow of R22 and nitrogen for the pyrolysis process in the formation of TFE was set to flow rates of 300 and 5000 cm^3/min, respectively. This process led to the synthesis of TFE, which flowed to the end parts of the production line and, finally, froze inside the U-trap, which was cooled with liquid nitrogen for an approximately 1.5-h time interval. Then, the two valves were closed, and the U-trap was disconnected from the production line.

Then, one of the valves was first connected to one end of the traps containing each type of solid support with silicone tubing. Afterward, to eliminate any memory effect related to the presence of nitrogen and air from the circulation line, the frozen TFE was allowed to flow through the solid supports for about 1 min.

Finally, the other valve was connected to the other end part of the trap containing the solid supports. This was put away for 48 h until the adsorption process was completed, whereas we controlled the

temperature of the U-trap to about −10°C by locating it inside a refrigerator.

For synthesis of the PTFE nanoparticles, several grams of each type of solid support were poured inside a copper cell. Then, the copper cell containing the solid support was positioned inside the sidearm of the system designed for the polymerization process. About 2 cm^3 of distilled water as an initiator was also added to the bottom of the sidearm of the designed system. The operating conditions, applied to the system for the polymerization process, were a temperature of 100°C and a pressure of 10^7 Pa.

RESULTS AND DISCUSSION

Optimization of the operating parameters

For maximum adsorption of TFE and to synthesize large amounts of PTFE nanoparticles on the surfaces of the different solid supports, the purity percentage of TFE was considered an important factor. To obtain pure TFE, several parameters, such as the flow rates of R22 and nitrogen gas, the temperature of the furnace, and the effect of liquid nitrogen, were optimized. Also, the optimum temperature and pressure were selected for the generation of the PTFE nanoparticles. For this purpose, the purity of the TFE was determined with the FTIR technique. Also, methods such as FTIR spectroscopy and TGA were considered as suitable experimental techniques for the quantitative evaluation of the adsorptive percentage of TFE and the degree of PTFE formed on each solid support. The sizes of the deposited PTFE nanoparticles were also evaluated with SEM, AFM, and XRD spectroscopy. The defects of each solid support were determined according to Raman spectroscopy. In the following sections, the optimization processes are discussed in detail.

In this study, FTIR spectroscopy was used to measure the performance of each stage. This technique is appropriate for estimating the rate and amount of TFE adsorbed on solid substrates.[33,34] In the FTIR spectra of TFE and PTFE, the CF_2 stretching vibration occurred as the most intense IR absorption band, near 1200 cm^{-1}. This band was multiple and consisted of three independent peaks positioned at 1240, 1215, and 1150 cm^{-1}. Other major bands were located at 641, 554, and 515 cm^{-1} and were assigned to the C—F bending modes. The IR absorption band at 2366 cm^{-1} was the overtone of CF_2 stretching vibrations. Also, the C—Cl stretching vibration was a strong absorption at 760–540 cm^{-1}.[33,34]

In this study, R22 was used for the pyrolysis process in the production of TFE as the monomer. R22 is a common reagent for the industrial production of TFE for synthesis of PTFE.[23] Usually, the pyrolysis process of R22 is performed directly at temperatures between 750 and 950°C or at a temperature of about 650°C with appropriate catalysts, such as metal fluoride.[35] Because TFE is unstable, it cannot be stored for a long time. Hence, it should be polymerized as soon as possible. Therefore, for the formation of PTFE, it is necessary to prepare TFE in an online system.[29] However, the main limitation of the general polymerization technique is that the produced PTFEs are often aggregated with each other to generate some bulky PTFE particles with a large size distribution.[36] This causes some difficulties in the synthesis of PTFE nanoparticles. Therefore, to solve this problem, a novel method was proposed to control the size of the PTFE nanoparticles via the surface adsorption of TFE on each solid support. In this study, for more simplicity, we aimed to optimize the parameters related to the synthesis of the TFE monomers without using any catalysts.

To optimize the temperature of the pyrolysis process, the amount and purity percentages of the TFEs, synthesized individually at different temperatures, including 600, 700, 950, and 1000°C, and also at a constant flow rate of 300 cm^3/min for R22 and 5000 cm^3/min for nitrogen gas were investigated with FTIR spectroscopy. The FTIR spectrum of TFE exhibited the maximum intensity for the CF_2 stretching vibrations at about 1288 cm^{-1} for TFE synthesized at temperatures between 900 and 1000°C. Therefore, 950°C was selected as the optimum temperature in the generation of the TFE monomer.

To optimize the flow rate of R22 in the pyrolysis process for the synthesis of the largest amounts of highly purified TFE, several TFE samples were synthesized at 950°C and at a constant flow rate of nitrogen (5000 cm^3/min) and different flow rates of R22, which ranged from 200 to 800 cm^3/min. The synthesized TFE samples were also analyzed with FTIR spectroscopy. Following the intensities of the absorption peaks related to the C—F and C—Cl bands at about 740 and 1200 cm^{-1}, respectively, revealed that the maximum suitable flow rate of R22 for the formation of TFE with the maximum purity percentage was observed at a flow rate of 300 cm^3/min for R22. Therefore, this value was selected as the optimum flow rate. Figure 3 shows the FTIR spectrum of the gaseous TFE sample as the monomer synthesized at 950°C and at an R22 flow rate of 300 cm^3/min.

Because HCl vapor is considered a byproduct in the synthetic process of TFE,[37] it is necessary to separate TFE from the HCl vapors. For this purpose, the synthesized TFE gaseous samples were bubbled into an aqueous basic solution. In this study, a solution of 5.0 mol/L NaOH was selected. Therefore, the HCl vapors were easily separated from TFE. However, this stage caused another difficulty. The bubbling of the TFE into the aqueous solution

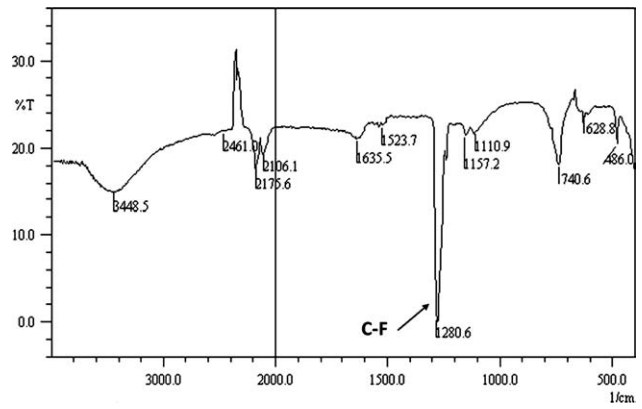

Figure 3 FTIR spectrum of the gaseous sample of TFE under the optimum conditions.

caused the TFE to be moistened with water vapors. The presence of water vapors in the TFE may have caused some limitations in the adsorptive behavior of TFE on the solid supports. In this study, water vapors were easily separated from TFE on the basis of the significant difference between the freezing points of TFE (−142.5°C) and water.[24] In this study, liquid nitrogen was used to preconcentrate the TFE and to separate the TFE from water and nitrogen.

Characterization of the TFE and PTFE/solid supports

The adsorptive behavior of TFE on different solid substrates, including CNFs, alumina, silica, PVP, molecular sieves, and activated carbon were investigated with the TGA instrumentation system. In this study, because the mechanism of the formation of the nanoparticles of fluoropolymers was based on the physisorption and chemisorption of TFE as the monomer, the selection of solid supports was based on the amounts of active surface area of each solid substrate and on the modification of the solid supports with some functional groups with which TFE could bond. To estimate the adsorption percentages on each solid substrate, a trace flow of TFE (2.0 cm^3/min) was passed through each solid support, and the changes in weight were recorded. The results were in accordance with the adsorption traces (as shown in Fig. 4) of TFE on each solid support. The physicochemical adsorptive behavior of TFE was clearly observed according to the adsorption traces (Fig. 4). On the basis of Figure 4, a significant adsorptive difference in the amounts of adsorbed TFE revealed the intrinsic property of each solid substrate for TFE adsorption. In this study, the maximum adsorption percentages were observed for the CNFs and PVP. The adsorption of TFE on the solid substrates such as PVP and alumina was also evidenced with FTIR spectroscopy, as shown in Figure 5. The results demonstrate that solid supports such as the CNFs, PVP, alumina, and silica were appropriate supports for the surface adsorption of TFE.

To further evaluate the amounts of the adsorption of the TFE on each solid support, TGA of TFE adsorbed on different solid substrates was performed in an inert atmosphere of nitrogen with a temperature ramp of 5.0°C/min. The TGA results of the TFE adsorbed on the different solid substrates were compared with each other, as shown in Figure 6. According to the thermograms (Fig. 6) of the TFE adsorbed on the solid substrates, a decrease in weight was observed at about 150°C. At this temperature, the previously adsorbed TFE was desorbed from the solid supports. As shown in Figure 6, dissimilar behaviors were observed for different solid supports, depending on the morphology of the substrate. Also, the plateau of the thermogram (the last part of each thermogram) showed the quantity of TFE and revealed the capacity of each solid substrate for the adsorption of TFE. This behavior was also considered more proof for the maximum capacity of the CNFs for the adsorption of TFE. Therefore, basal planes of solid supports with a high active surface area, such as CNFs, operate as appropriate substrates for the adsorption of TFE. Also, the roughness of the solid support acted as proper substrate for the nucleation process in the synthesis of the fluoropolymer nanoparticles.

For the polymerization process, the TFE deposited on each solid support was polymerized. In the polymerization process, the reported conditions for the synthesis of PTFE were a temperature of about 100°C and a pressure of about 10^7 Pa.[36] In this study, the same conditions were selected for the synthesis of the PTFE nanoparticles.

In formation of the PTFE nanoparticles, water vapors acted as an initiator.[29] It seemed that the

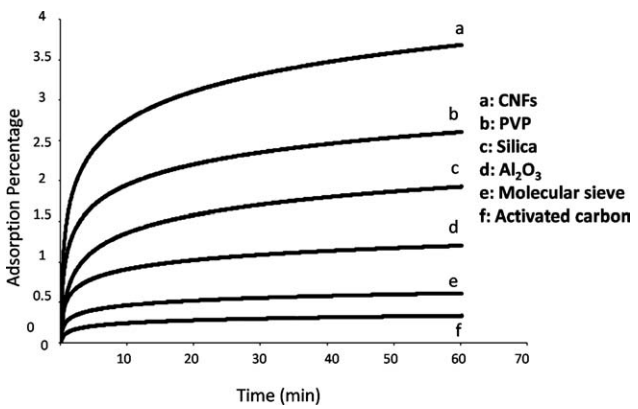

Figure 4 Adsorptive behavior of TFE on the (a) CNFs, (b) PVP, (c) silica, (d) Al_2O_3, (e) molecular sieve, and (f) activated carbon with a TGA instrumentation system.

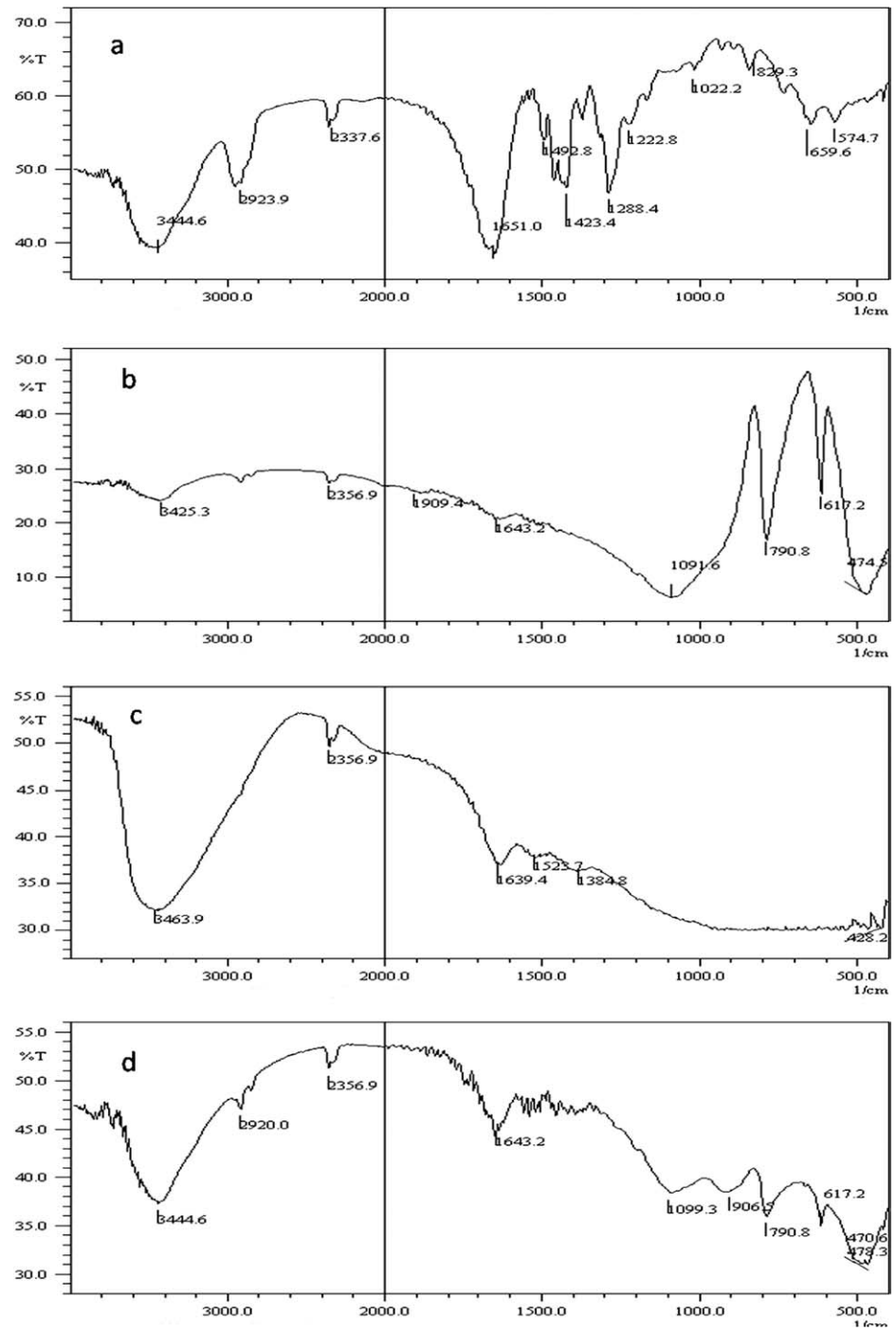

Figure 5 FTIR spectra of the solid supports on a 100-fold excess of KBr for (a) pure PVP, (b) PVP adsorbed with TFE, (c) alumina, and (d) alumina adsorbed with TFE.

amounts of adsorbed TFE on each solid supports had a strong influence on the growth and termination reactions of the PTFE nanoparticles.

The diameter of the PTFE nanoparticles depended on the size and morphology of the solid substrate on which the TFE was adsorbed. Solid substrates, such as the CNFs, silica, alumina, molecular sieves, and activated carbon, had various surface-to-volume ratios (aspect ratios). In this study, the maximum adsorption of TFE was evaluated for CNFs. Also, spherical PTFE nanoparticles were clearly observed according to the SEM (Fig. 7) and AFM images (Fig. 8) on highly orientated pyrolytic graphite. The shape of the synthesized PTFE nanoparticles was similar to those from a procedure reported previously for the synthesis of PTFE nanoparticles.[20,32] The smallest PTFE nanoparticles were also observed for the CNFs according to the SEM and AFM

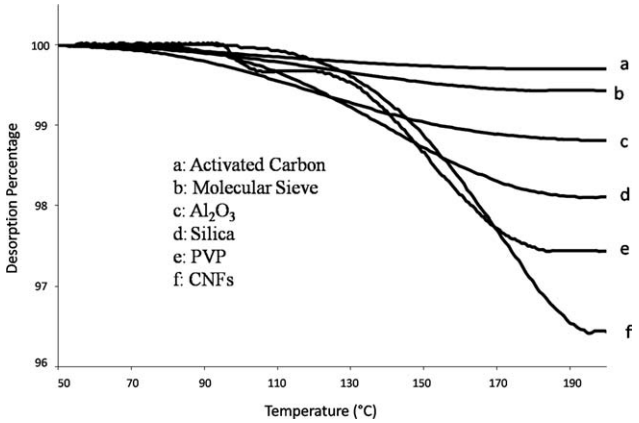

Figure 6 TGA of deposited TFE on different solid supports.

images. The inset of Figure 7 shows the homogeneous distribution of the PTFE nanoparticles on the CNFs. Also, the histogram shown in Figure 9 presents the average frequency distribution of the different sizes of synthesized PTFE nanoparticles on the CNFs on the basis of the AFM image.

The XRD patterns of PTFE on different solid substrates are also shown in Figure 10. According to the XRD patterns, the strong peaks at $2\theta = 30^\circ$ corresponded to the PTFE nanoparticles. The size of the PTFE nanoparticles was also determined from X-ray line broadening with the Debye–Scherrer equation as follows: $D = 0.9\ \lambda/\beta \cos\theta$, where D is the average crystalline size, λ is the X-ray wavelength used, β is the angular line width at half-maximum intensity, and θ is Bragg's angle. According to the peaks of the PTFE nanoparticles corresponding to $2\theta = 30^\circ$ and $\lambda = 1.5473$ Å, the average sizes of PTFE nanoparticles on different solid substrates were estimated to about 90 nm for the CNF support, 130 nm for PVP, 150 nm for alumina, and about 200 nm for silica; this indicated good agreement among

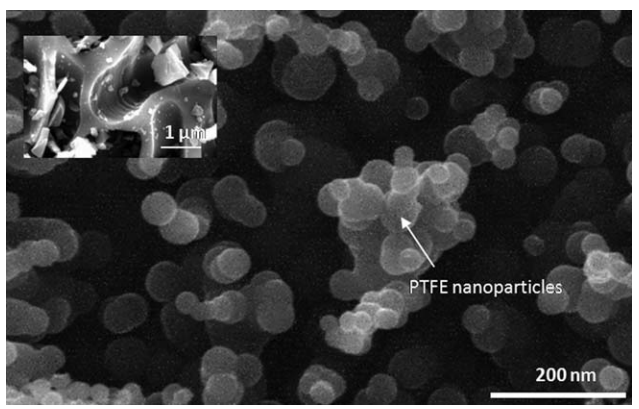

Figure 7 SEM images of the PTFE nanoparticles on the CNFs. Inset: SEM micrograph showing the homogeneous distribution of the PTFE nanoparticles on the CNFs.

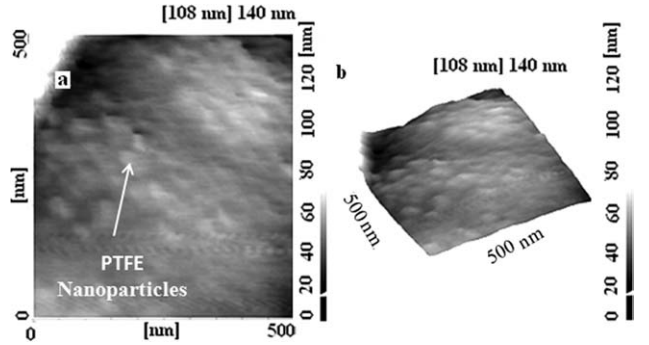

Figure 8 High-resolution AFM images: (a) two-dimensional and (b) three-dimensional images of PTFE on the CNFs.

the sizes evaluated from XRD spectroscopy and the AFM images.

TGA illustrated that the quantities of the PTFE nanoparticles on each solid substrate were 3.53 ± 0.09% for the CNFs, 2.31 ± 0.10% for PVP, 2.11 ± 0.12% for silica, and 0.97 ± 0.16% for alumina. These results refer to the various capacities for the adsorption of TFE in formation of the PTFE nanoparticles. Also, carbon nanomaterials have so a high specific surface area that they act as suitable substrates for the adsorption of the largest amounts of TFE. The evaluation of the amounts of PTFE nanoparticles formed on each indicated that a higher percentage of PTFE nanoparticles deposited on the CNFs. Obviously, this was due to the narrow size distribution and the high aspect ratio of the CNFs, which provided a higher aspect ratio for the formation of the PTFE nanoparticles. In addition, the high active surface area and the tubular construction of the CNFs as a support promoted the adsorption of TFE on the active regions.[38] Also, the unique properties of carbon nanostructures such as CNFs delays the mass-transfer limitations of the TFE adsorptive process.[39]

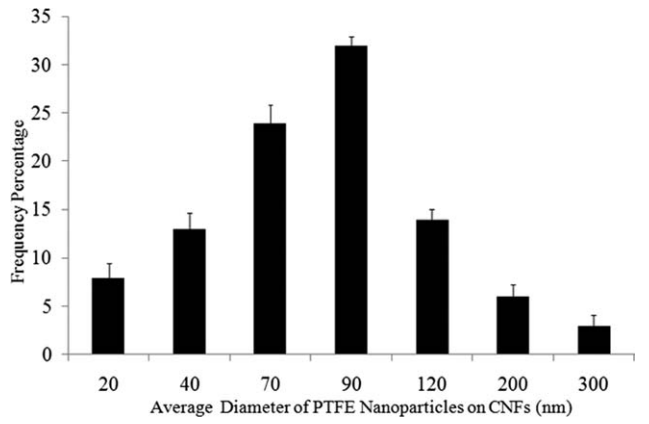

Figure 9 Histogram showing the distribution of the PTFE nanoparticles on the CNFs.

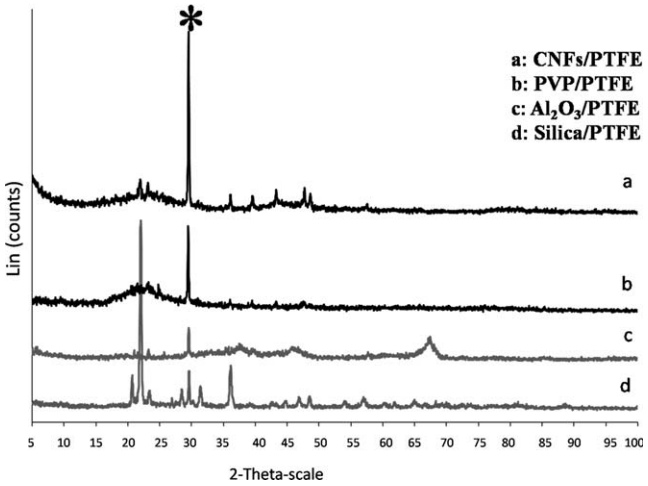

Figure 10 XRD patterns of the PTFE nanoparticles on different solid supports, including the (a) CNFs, (b) PVP, (c) Al_2O_3, and (d) silica.

In addition, the adsorption and diffusion of TFE on the different layers of each solid support had a direct correlation with the square of the defect extent of each solid support, as indicated by the Knudsen equation.[40] Raman spectroscopy of the CNFs demonstrated tangential mode (1450–1650 cm^{-1}) and disorder mode (1250–1350 cm^{-1}), and their ratio indicated the degree of defect extent of the CNFs.[41] In this study, the maximum defect extent (4.84) was estimated for CNFs on the basis of Raman spectroscopy;[41] this revealed the normal distribution of PTFE in the CNF matrix. Thus, the adsorptive capability of the solid support was influenced by the defect extent of the nanostructures as the solid support during the formation of PTFE. Commonly solid substrates with higher surface roughnesses, such as CNFs, provide stronger interactions with the adsorbed species.[42,43] Therefore, the presence of plenty of adsorptive sites in the structure of nanomaterials such as CNFs causes the adsorption of large amounts of TFE.[42,43] In this study, the results attained from various analytical techniques were in good agreement with the degree of the defect extent of nanostructures such as CNFs.

However, the aim of this study was the synthesis of PTFE nanoparticles doped on a solid support, but in some practical industrial uses of PTFE nanoparticles, the sonication of a PTFE-doped solid support in a sonication bath containing a suitable surfactant easily results in the separation and codeposition PFTE particles.[44]

CONCLUSIONS

Depending on the degree of the defect extent and the morphology of each solid support, solid materials have different capacities for the formation of PTFE nanoparticles. The amounts and the sizes of synthesized PTFE nanoparticles depended on the characteristics of the solid substrate. The exceptional properties of carbon nanostructures such as CNFs as solid substrates acted as a suitable solid support for the surface adsorption of TFE as a monomer. The aspect ratio of the solid substrates was also considered an important factor in the adsorptive process of TFE, followed by the formation of the PTFE nanoparticles.

The importance of the deposition of PTFE on different solid supports has been examined in different parts of industry over recent years.[45–49] Recently, supercapacitors have attracted great attention because of their high capacitance and potential applications in electronic devices. One popular material for the preparation of supercapacitors is CNFs, which provide lots of edge sites on the outer wall. Today, to obtain a higher specific surface area, rational pore distribution or binding CNFs for double-layer capacitors, some modification of CNFs must be done. However, chemical vapor deposition is one of the most common methods to modify CNFs, but in this approach, we lose some of porosity of CNFs. PTFE is the main material used as a binder in double-layer capacitors. As shown in our investigated approach, the PTFE nanoparticles doped on the CNFs could easily be used as binders without a loss in the porosity of the CNFs in the fabrication of higher supercapacitors. We propose that the procedure reported in this article could easily be used for the homogeneous and regular deposition of PTFE on different solid supports. The proposed procedure would promote the efficiency and performance of solid supports in different fields of science. We also intend to investigate the chemical reactions between TFE and different solid substrates, such as PVP, during TFE polymerization.

The authors thank to M. Hemmatian for his kind help in designing the instrumentation systems. The authors also thank K. Moradi for his revision.

References

1. Reisinger, J. J.; Hillmyer, M. A. Prog Polym Sci 2002, 27, 971.
2. Tu, C.-Y.; Liu, Y.-L.; Lee, K.-R.; Lai, J.-Y. Polymer 2005, 46, 6976.
3. Simon, C. M.; Kaminsky, W. Polym Degrad Stab 1998, 62, 1.
4. Kim, J.-H.; Kawai, M.; Yonezawa, S.; Takashima, M. J Fluorine Chem 2008, 129, 654.
5. Vanswijgenhoven, E.; Cutulic, S.; Kenis, K.; Regter, G. D.; Crols, O.; Pennings, P. Wear 2008, 264, 494.
6. Borkar, S.; Gu, B.; Dirmyer, M.; Delicado, R.; Sen, A.; Jackson, B. R.; Badding, J. V. Polymer 2006, 47, 8337.
7. Show, Y.; Itabashi, H. Diamond Relat Mater 2008, 17, 602.
8. Murali, K. P.; Rajesh, S.; Prakash, O.; Kulkarni, A. R.; Ratheesh, R. Compos A 2009, 40, 1179.
9. Aderikha, V. N.; Shapovalov, V. A. Wear 2010, 268, 1455.

10. Krishnamurthy, B.; Deepalochani, S. Int J Hydrogen Energy 2009, 34, 446.
11. Xiang, D.; Shu, W.; Li, K. Mater Sci Eng A 2008, 483–484, 365.
12. Dascalescu, D.; Polychronopoulou, K.; Polycarpou, A. A. Surf Coat Tech 2009, 204, 319.
13. Lai, J.-Y.; Hsiue, G.-H. React Funct Polym 2007, 67, 1281.
14. Zhao, Q.; Liu, Y. J Food Eng 2006, 72, 266.
15. Bao, D.; Cheng, X. J. Rare Earth 2006, 24, 564.
16. Zhang, Z.; Chen, X. Polym Test 2009, 28, 288.
17. Bamperng, S.; Suwannachart, T.; Atchariyawut, S.; Jiraratananon, R. Sep Purif Technol 2010, 72, 186.
18. Rico, E. F.; Minondo, I.; Cuervo, D. G. Wear 2009, 266, 671.
19. Menini, R.; Farzaneh, M. Surf Coat Tech 2009, 203, 1941.
20. Burkarter, E.; Saul, C. K.; Thomazi, F.; Cruz, N. C.; Roman, L. S.; Schreiner, W. H. Surf Coat Technol 2007, 202, 194.
21. Sawada, S.-I.; Yamaki, T.; Nishimura, H.; Asano, M.; Suzuki, A.; Terai, T.; Maekawa, Y. Solid State Ionics 2008, 179, 1611.
22. Dumitras, M.; Odochian, L. J Therm Anal Cal 2002, 69, 599.
23. Sung, D. J.; Moon, D. J.; Moon, S.; Kim, J.; Hong, S.-I. Appl Catal A 2005, 292, 130.
24. Dhoot, S. N.; Freeman, B. D.; Stewart, M. E. In Encyclopedia of Polymer Science and Technology; Mark, H. F., Ed.; Wiley: Hoboken, NJ, 2004; Vol. 3, p 378.
25. Tian, Z. Q.; Wang, X. L.; Zhang, H. M.; Yi, B. L.; Jiang, S. P. Electrochem Commun 2006, 8, 1158.
26. Yasuoka, H.; Yoshida, M.; Sugita, K.; Ohdaira, K.; Murata, H.; Matsumura, H. Thin Solid Films 2008, 516, 687.
27. Yu, C.-H.; Kusumawardhana, I.; Lai, J.-Y.; Liu, Y.-L. J Colloid Interface Sci 2009, 336, 260.
28. Ikeda, S.; Tabata, Y.; Suzuki, H.; Miyoshi, T.; Katsumura, Y. Radiat Phys Chem 2008, 77, 401.
29. Ebnesajjad, S. In Fluoroplastics: Non-Melt Processible Fluoroplastics. Vol. 1; William Andrew: New York, 2000.
30. Sato, C.; Ohtani, T.; Nishitani, H. Comput Chem Eng 2000, 24, 945.
31. Lu, X.; Wong, K. C.; Wong, P. C.; Mitchell, K. A. R.; Cotter, J.; Eadie, D. T. Wear 2006, 261, 1155.
32. Rico, E. F.; Minondo, I.; Cuervo, D. G. Wear 2007, 262, 1399.
33. Thompson, C. D.; Robertson, E. G. McNaughton,D. Chem Phys 2002, 279, 239.
34. Cui, X.; Zhong, S.; Xu, J.; Wang, H. Prog Colloid Polym Sci 2007, 285, 935.
35. Sung, D. J.; Moon, D. J.; Kim, J.; Moon, S.; Hong, S.-I. Stud Surf Sci Catal 2006, 159, 233.
36. Schwartz, S. S.; Goodman, S. H. In Plastics Materials and Processes; Van Nostrand Reinhold, Company Inc.: New York, 1982; Chapter 2.
37. Morato, A.; Alonso, C.; Medina, F.; Salagre, P.; Sueiras, J. E.; Terrado, R.; Giralt, A. Appl Catal B 1999, 23, 175.
38. Chen, Y. L.; Liu, B.; Wu, J.; Huang, Y.; Jiang, H.; Hwang, K. C. J Mech Phys Solids 2008, 56, 3224.
39. Díaz, E.; Ordóñez, S.; Vega, A. J Colloid Interface Sci 2007, 305, 7.
40. Satterfield, C. N. In Mass Transfer in Heterogeneous Catalysis; MIT Press: Cambridge, MA, 1970.
41. Byon, H. R.; Hyunseob, L.; Song, H. J.; Choi, H. C. Bull Korean Chem Soc 2007, 28, 2056.
42. Akbulut, M.; Alig, A. R. G.; Israelachvili, J. J Chem Phys 2006, 124, 174703-1.
43. Raja, P.; Bensimon, M.; Klehm, U.; Albers, P.; Laub, D.; Kiwi-Minsker, L.; Renken, A.; Kiwi, J. J Photochem Photobiol A Chem 2007, 187, 332.
44. Ger, M.-D.; Hwang, B. J. Mater Chem Phys 2002, 76, 38.
45. Balaji, R.; Pushpavanam, M.; Kumar, K. Y.; Subramanian, K. Surf Coat Tech 2006, 201, 3205.
46. Rajesh, S.; Nisa, V. S.; Murali, K. P.; Ratheesh, R. J Alloy Compd 2009, 477, 677.
47. Chebbi, R.; Beicha, A.; Daud, W. R. W.; Zaamouche, R. Appl Surf Sci 2009, 255, 6367.
48. Luo, Z.; Zhang, Z.; Wang, W.; Liu, W.; Xue, Q. Mater Chem Phys 2010, 119, 40.
49. Zarei, M.; Salari, D.; Niaei, A.; Khataee, A. Electrochim Acta 2009, 54, 6651.